Chapter 1

Advances in Scanning Thermal Microscopy Measurements for Thin Films

Liliana Vera-Londono, Olga Caballero-Calero, Jaime Andrés Pérez-Taborda and Marisol Martín-González

Additional information is available at the end of the chapter

http://dx.doi.org/10.5772/intechopen.79961

Book title: Coatings and Thin-Film Technologies
IntechOpen, January 2019
Book ISBNs 978-1-78984-870-0, 978-1-78984-871-7

Abstract

One of the main challenges nowadays concerning nanostructured materials is the understanding of the heat transfer mechanisms, which are of the utmost relevance for many specific applications. There are different methods to characterize thermal conductivity at the nanoscale and in films, but in most cases, metrology, good resolution, fast time acquisition, and sample preparation are the issues. In this chapter, we will discuss one of the most fascinating techniques used for thermal characterization, the scanning thermal microscopy (SThM), which can provide simultaneously topographic and thermal information of the samples under study with nanometer resolution and with virtually no sample preparation needed. This method is based on using a nanothermometer, which can also be used as heater element, integrated into an atomic force microscope (AFM) cantilever. The chapter will start with a historical introduction of the technique, followed by the different kinds of probes and operation modes that can be used. Then, some of the equations and heating models used to extract the thermal conductivity from these measurements will be briefly discussed. Finally, different examples of actual measurements performed on films will be shown. Most of these results deal with thermoelectric thin films, where the thermal conductivity characterization is one of the most important parameters to optimize their performance for real applications.

Keywords: scanning thermal microscopy, thermal probes, thermoelectric thin films, thermal conductivity, local temperature measurements

1. Introduction

In the last years, there has been a great improvement in thin film fabrication, with a reduction in the costs, and an enhancement in their quality and performance, as it is shown in the different chapters of this book. Therefore, there has been an increase in thin film applications in different fields [1], which take advantage of the modification of electronic and thermal transport when the dimensions of the material are reduced to lengths comparable to the mean free path of phonons and charge carriers. Thin films with tailored thermal and electrical properties are employed in solar cells [2], electronics [3], or thermoelectric conversion devices [4], among other fields. Nevertheless, the optimization of the materials for these applications requires measurement techniques that provide precise information of both the surface and the properties at the nanoscale, with high local resolution. In this sense, scanning probe microscopy (SPM) methods fulfill these requirements, with a high spatial resolution, strong sensitivity, and in most cases, no previous preparation of the sample is needed. In this chapter, we will focus on one type of SPM technique, namely scanning thermal microscopy (SThM). This technique allows to study the thermal transport phenomena at the nanoscale, providing a powerful tool to understand thermal properties of thin films.

Historically, the atomic force microscope (AFM) was developed by Binning et al. [5] in 1986. The AFM was a new type of microscope that used the principles of the scanning tunneling microscope (STM) and the stylus profilometer (SP), allowing the investigation of both conductors and insulators at the atomic scale (which could not be characterized by STM before) by measuring interatomic and electromagnetic forces. Controlling the probe-sample gap by a feedback loop that kept constant the force between the probe and the sample during the scan, the topography of the sample was obtained from a contrast image given by the height of the probe at each point. In the same year, only a few months later, a new noncontact high-resolution surface characterization technique for topographic images was presented by Williams and Wickramasinghe [6], the scanning thermal profiler (STP). This was the beginning of the scanning thermal microscopy. In this case, the probe was conical, with a thermocouple nanojunction located at the end of its tip. The probe was then heated with a laser and brought close to the surface of the sample, where it was cooled down due to the heat transfer to the sample. In this case, the temperature of the probe was used in the feedback loop to control the gap between tip and sample, keeping the probe temperature constant while varying its height. Therefore, this information could not be used to provide thermal maps of the surface, but that was not the objective of this technique, which tried to improve the topographic images obtained by using the thermal interaction between the tip and the sample. In the next few years, different techniques based on probe scanning microscopies were developed to measure a variety of properties in the micro- and nanoscale: the scanning tunneling thermometer, which was able to measure with 1 nm spatial resolution the optical absorption of thin metal films, or to map the variations of the electrochemical potential at the nanometer scale [7, 8]; the so-called Kelvin probe force microscopy (KPFM), which provided the work function or surface potential of a sample [9], through the measurement of the contact potential differences. This principle was also used while scanning the surface with a heated sharp probe, obtaining a qualitative image of the changes at the subsurface on the thermal conductivity [10]. In this last

work, dated in 1992, Nonnemacher and Wickramasinghe defined this period of time as one with "a tremendous growth in scanned probe microscopies" [10].

The next breakthrough in the field took place in 1993 when Majumdar et al. went a step further. They replaced the AFM probe by two wires (chromel and alumel) to form a thermocouple junction at the tip and, when scanning the surface with this modified probe, they obtained simultaneously the thermal and topographical images with a sub-micrometric spatial resolution [11]. From this moment on, different groups started working on improvements on this type of measurements, such as Pylkki et al., who integrated a resistive thermal probe within an AFM cantilever, in order to measure both the actual temperature and the thermal conductivity [12]. These kinds of probes can work in two different modes, passive (where they act as a thermometer) or active (acting also as a heater), which will be discussed in detail later (Section 2). In the case of the first thermistor probe, the temperature of the probe was monitored by measuring the changes in its electrical resistance [12]. Further works explored the potential of this scanning thermal microscopy (SThM) technique to study the thermal response of thin films and nanostructures, using different designs for the AFM probes modified with a thermocouple to minimize the image distortion, temperature loss and, at the same time, increase the imaging resolution, as it was made by Majumdar et al. [13]. Nevertheless, it is worth to note that, at this point, the results obtained as far as the thermal properties were concerned, were more qualitative than quantitative, given that the models used were quite simple and did not take into account the geometry of the probes or the heat transfer characteristics when working in contact or noncontact modes. One of the first quantitative results was obtained in 1995 by Hammiche et al. They presented a work based on SThM performed with a Wollaston cantilever (please see Section 2) to obtain subsurface imaging of copper metallic particles embedded in polystyrene [14]. The thermal image was acquired in active mode, keeping the temperature of the probe constant. In this mode, the probe acts as a resistive heater that forms part of a Wheatstone bridge that, thanks to a feedback system, gives the appropriate voltage to maintain a constant temperature of the probe. In this work, they also developed a one-dimensional theoretical model to obtain quantitative information from the thermal maps, obtaining information of the depth at which the inclusions were, and thermal conductivity inhomogeneities. Although the results obtained did not match the expected thermal conductivity values and the precision of the location of the buried particles was very low, this was probably due to a too simple heat transfer model. But this paved the way for further and better theoretical models for these systems.

The SThM started to be present in overview articles of thermal analysis in the following years, such as that published by Kölzer et al. [15], where different techniques used for thermal imaging of electronic devices were reviewed. The influence of thermal stresses in the performance and reliability of electronics, and thus the thermal characterization of micro- and nanoelectronic devices, is quite relevant to carry out the device optimization and avoid malfunctioning due to a bad management of heat. Among the different methods cited (thermography, optical beam displacement, thermoreflectance, etc.), near-field techniques as SThM were discussed as the best method to achieve the characterization at the micro- and nanoscale at high resolution (achieving down to 30 nm lateral resolution). In 1998, Gmelin et al. presented a review article on the evolution of SThM [16], which together with the extensive review written by Majumdar in

1999 [17] gives a complete overview of the state of the art of this method at the end of the twentieth century. At that point, the SThM technology was used for the thermal analysis of micro- and nanostructured materials and devices. In fact, Majumdar made a distinction between three different categories: SThM based in thermo-voltage, electrical resistance, and thermal expansion measurements. In this review, the different probes, experimental setups and specific applications for each of them are discussed. One of the most important issues to interpret the measurements performed by SThM is to understand the fundamental heat transfer phenomena between the tip and the sample, which controls the resolution, accuracy, and artifacts. Therefore, the mechanics of heat transfer are also reviewed in depth in this work.

A further breakthrough in SThM was achieved in 1999 by Fieged et al. when they combined an SThM with the 3ω method in order to obtain quantitative thermal conductivity measurements with high accuracy (less than 2% deviation), using a resistive probe as heater and thermometer element [18]. The 3ω method was first used for thermal conductivity measurements by Cahill and Pohl in 1987 [19], using a single element as both heater and thermometer. This method was developed in close relation to the hot-wire and hot-strip methods for thermal conductivity measurement, but with the main difference of using the frequency domain instead of the time domain, thanks to the use of a lock-in amplifier. In brief, the 3ω method applied to the SThM (known as 3ω-SThM) can be understood as follows: a thermistor probe is connected to an alternating current (AC) at an angular frequency ω. This current will produce a heating of the probe by Joule effect, which will go as the square of the current, that is, with a 2ω frequency. Then, it will exchange heat with the ambient and with the surface of the sample, producing a temperature oscillation. The rate of the heat transfer between the probe and the sample depends on the thermal conductivity of the sample. Being the probe a thermistor, the changes in its temperature will produce a change in its resistance at the same frequency, that is, at 2ω. Finally, the total voltage will be proportional to the product of the resistance fluctuation at 2ω and the excitation current at ω, that is, the voltage will oscillate at a frequency of 3ω. Then, the amplitude of this voltage is measured by a lock-in amplifier and processed. The 3ω-SThM has been employed in several works, along with experimental improvements, and an important effort in the development of theoretical models was also performed in the following years [20–24].

The latest improvements in the SThM technique have come from studying in depth on how different materials react to local temperature rises. The heat transfer mechanisms that have to be taken into account can be divided into solid-solid conduction between the tip and the sample in contact; liquid conduction (if certain humidity which takes place in the real measurements and formed liquid meniscus around the tip is present) and gas conduction (when heat is transferred through the surrounding atmosphere from the tip to sample). One example of these models, where the surrounding gas around the tip and the sample is taken into account, shows how these effects can distort the thermal signal and diminish the spatial resolution [25]. Therefore, experiments performed in vacuum were carried out. Nowadays, SThM has evolved and is currently applied to many different micro- and nanosystems. Thermal models to better understand the thermal transport and heat transfer mechanisms at the micro- and nanoscale and how these influence the measurements, along with novel calibration techniques to achieve better results, have been developed [26, 27]. These have also contributed to a better understanding of the technique and to obtain quantitative measurements. Another

method proposed in 2008 to perform measurements in ambient condition, was proposed using a double scan technique [28]. Most of these contributions can be separated in applications to 1D structures, such as nanowires [29, 30] or carbon nanotubes [31, 32], 3D materials [33], thin films [34] (which are the objective of the present chapter), and in the last years, the SThM technique has also been successfully applied to the study of the emerging field of 2D materials [35].

As it was aforementioned, in this chapter, we will explore the characterization of the thermal conductivity of thin films by SThM. Firstly, we will discuss the different operational modes of the probe along with an overview of different kinds of probes that can be used, their applications, and their limitations. Then, we will focus on two different types of heating mechanisms (AC and DC) implemented in thermistor probes, along with their theoretical models. Finally, we will review some experimental results, most of them from our own group, devoted to extract the thermal conductivity from the thermal response of SThM measurements in thermoelectric thin films. For thermoelectric applications, where temperature gradients are converted into electricity by the thermoelectric (TE) effect, the accurate characterization of the actual thermal conductivity of thin films is fundamental to optimize their performance. The most efficient TE materials are those which exhibit both high Seebeck coefficient and electrical conductivity along with reduced thermal conductivity. One way of reducing the thermal conductivity of a bulk material without affecting the transport properties is through reducing its dimensionality [36], such as preparing thin films. This thermal conductivity reduction has been reported for several materials, such as SiGe [37–39] Cu_2Se [40] and Ag_2Se [41] films, among others.

2. Thermal probes: operational modes and types

As it was mentioned in the Introduction, once the SThM probe approaches the surface of the sample and heat starts to be transferred, there are two different modes of operation: passive or active. On the one hand, in the passive mode, the temperature of the probe is monitored while scanning the surface, thanks to a constant current that passes through it. This provides a way to detect changes in the temperature of the probe, but this current must be also small enough to avoid self-heating. This measurement mode was implemented by Majumdar in 1993 [11]. On the other hand, the active mode implies that high currents pass through the probe, in order to be heated by Joule effect. Then, part of this heat will flow to the sample and this heat flow will depend on the thermal conductivity of the sample and the temperature difference. Therefore, in this mode, the probe is behaving as a heater. But, it also acts as a thermometer, given that the temperature is monitored by measuring the voltage of the probe, and this can be related to the thermal conductivity of the sample. This active mode can also be divided into two different operation modes: operation at constant current or at constant temperature [12]. In the first case, the active probe is connected to a constant current and the heat flux between the probe and the sample is detected by changes in the resistance of the probe. In the second case, the active probe works at a constant temperature by changing the applied voltage in the probe to keep its electrical resistance constant. This last operation mode is known as active mode at a

constant temperature. This mode has the fastest time response to reach local thermal equilibrium to operate.

These measurements can be done with a variety of probes. We will introduce two of the most used kinds of probes: thermoelectric and thermistor. At the end of the section, the main characteristics of those probes will be shown in **Table 1**.

2.1. Thermoelectric probes

The first type of thermal probe developed was a thermocouple placed at the end of a tungsten STM tip, used by Williams [6] and Majumdar [11], to study temperatures of nonconductive surfaces. These probes are being improved, and their properties are still under study. For instance, to know if the contribution of radiative heat transfer between a SiO_2-coated TE tip and the SiN_x-coated sample is negligible when compared with conductive heat transported by solid contact [42]. In general, thermoelectric (TE) probes have a nanoscale thermocouple junction at the tip. Further experimental and theoretical efforts were focused in obtaining thermal images in the sub-100 nm of spatial resolution using a thin-film thermocouple junction at the tip end [43]. New design and batch-fabricated TE probes were proposed in [44], to simultaneously improve the thermal sensitivity, the tip radius, and the thermal time constant (see the scheme in **Table 2**). In general, these tips can be used in active or passive mode, and are quite adequate to study heat dissipation, temperature distribution, and thermoelectric properties of both materials and devices. As far as the geometry and materials of these kinds of tips, the cone is around 8 μm in height and 8 μm in width at the base, and it has to be made of a low-thermal-conductivity material, such as silicon dioxide (SiO_2), to avoid heat losses from the TE junction to the cantilever. Then, the thermocouple junction films located at end of the tip are usually around 200 nm and the metals used for the junction are typically gold and chromium, isolated from each other along the probe with a Si_3N_4 film (see **Figure 1**).

With these kinds of probes, apart from studying the heat transport in different samples, other thermal properties, such as the interfacial thermal resistance, can be determined with the appropriate experimental setup and theoretical models. For instance, in Refs. [45, 46], these probes were used in active mode and through the measurement of the 2ω signal, they obtained thermoelectric properties of the samples. To this end, they heated the sample with a Peltier element, while the TE probe was Joule heating and scanning the sample. The analysis of the recorded signal was made by a steady periodic electrothermal model to obtain the thermoelectric parameters of the sample. Some disadvantages that these probes present is a low thermal sensitivity, which makes the temperature profiles obtained with them rather noisy. The resolution can be improved in vacuum, but working in these conditions can affect the temperature gradient. Also, it is necessary to include a circuit and a modified setup for some measurements, which complicates both the experimental implementation and the theoretical models needed to extract the properties [44].

2.2. Thermistor probes

Thermistor probes were introduced by Pylkki et al. [12] in 1994. These probes have a thermistor element, which can be a metallic thin film, a wire, or a highly doped semiconductor. This

Specifications	SThM probes			
	Thermoelectric	Thermoresistive		Semiconductor
	Thermocouple junction	Thermocouple Wollaston wire probe	Thermistor Pd/ Si_3N_4 probe	Doped silicon resistor probes
Operation modes				
Passive	At constant temperature			
Active		At constant current	At constant current	At constant current
Thermal properties extracted				
	Thermal conductivity, TE properties	Thermal conductivity, Seebeck	Thermal conductivity, Seebeck	Nanolithography, nano-LTA, glass transition, melting temperature
Probe characteristics				
Cantilever materials	Si_3N_4 SiO_2, Si	Ag shell Al mirror	Si_3N_4 NiCr limiters Au pads	Silicon (highly doped)
Spring Constant (Nm^{-1})	0.35	5	0.5	1
Tip materials	Au, Cr	Pt_{90}/Rd_{10}	Pd	Silicon low doped
Tip height (μm)	0.1	100	10	
Tip radius (μm)	0.065–0.1	≈2.5	<0.1	0.01–0.02
Electrical properties				
Nominal electrical resistance of the probe (Ω)	≈600	≈2	≈350	≈500
Thermal properties				
Max. temperature ($^{\circ}$C)	600–800	100	160	1000
Temperature coefficient resistance (K^{-1})		0.00165	0.0012	
Thermal cutoff frequency 2 fc (Hz)		250	2750	
Resolution				
Thermal lateral resolution (μm)		1–2	0.060–0.100	
Topographic lateral resolution (μm)	<0.03	<1	0.030–0.060	0.1

Table 1. Summary of the properties of the different SThM probes mentioned in the text.

thermistor varies its resistance with temperature. Therefore, the temperature of the probe can be monitored by recording its change in electrical resistance. Since then, the field of thermistor probes has evolved, and here, we will introduce different types, which have been commercially

Probe scheme	Advantages	Disadvantages
Wollaston wire 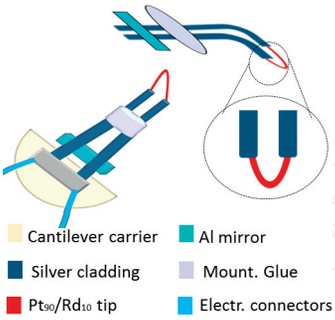 	• Known since 1994 (extensively used for heat transfer studies) • Theoretical works available on contact and noncontact mode • Implemented to act as thermometers and heaters • Endurable (it is difficult to mechanically break it)	• Bending issues: the angle of the V-shape can change after certain uses giving reproducibility issues. • No commercially available (Bruker does not sell them anymore) • After a certain number of scans, it is quite probable to have the wire dirty (dust or particles)
Microfabricated metal thin film 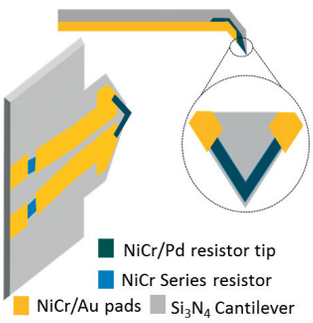 	• High thermal and topographic resolution (down to 100 nm) • High cutoff frequency: better for AC heating mode. • Reduced time image acquisition. • Commercially available • Batch fabricated • High sensitivity • More used in active mode	• High static sensitivity: easy electrical breakdown. • Higher price than normal probes. • Complex calibration steps and models for AC heating
Microfabricated thermoelectric 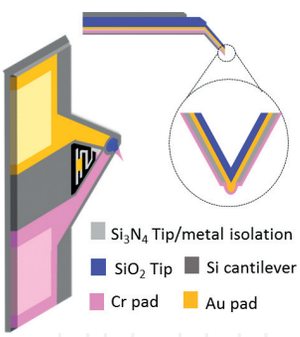 	• High thermal and topographic resolution (down to 50 nm) • Commercially available • Batch fabricated • High electrical resistance • More used in passive mode (but also used in active mode) • Robustness and high durability can be found with reasonable cost	• If the thermal sensitivity is not high, temperature profile can be noisy • For some experiments, a new setup and circuit may be necessary making complex the experimental and theoretical development • To obtain better resolution vacuum condition can be useful, but this can affect the temperature gradient
Microfabricated semiconductor 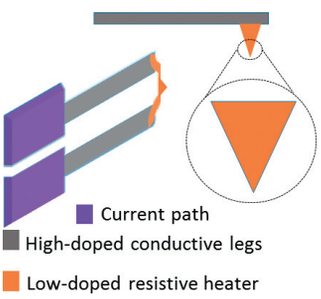 	• High thermal and topographic resolution (down to 100 nm) • Commercially available, reduced cost • Batch fabricated • High temperatures achieved (up to 1000°C) at the tip • High electrical resistance • More used in active mode	• No linear relation between temperature and electrical resistivity • High thermal constant resistances: difficult to extract quantitative measurements • Thermal bending

Table 2. Summary of advantages and disadvantages of the different thermistor types of probes discussed in this section.

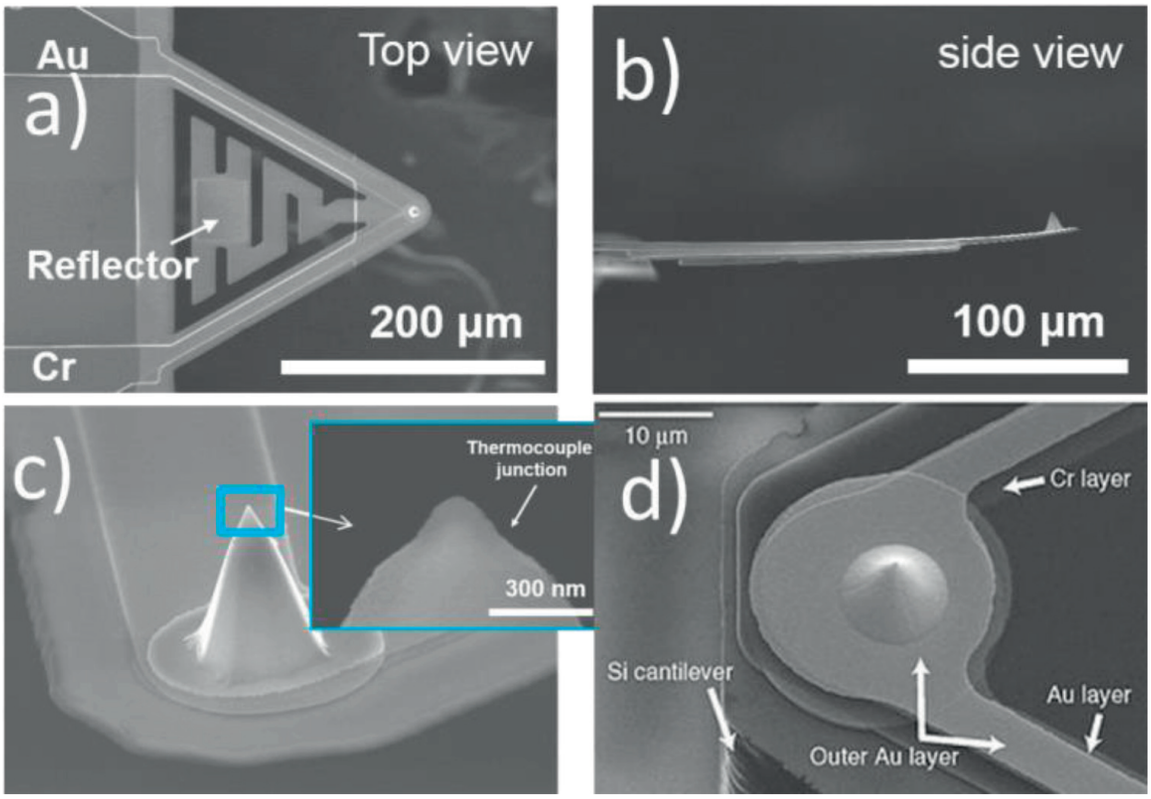

Figure 1. (a) SEM image with the top view of TE probe. (b) Side view of the probe. (c and d) SEM images at different magnifications of the tip. In (c), the detail of the thermocouple junction can be seen; (a), (b), and (c) are taken from http://www.tspnano.com of TSP Nanoscopy, and (d) is taken from [47].

implemented: Wollaston wire, microfabricated (Pd/SiN), and highly doped semiconductor probes. A summary of the advantages and disadvantages of each of the thermistor probes is shown in **Table 2**.

2.2.1. Wollaston probe

The Wollaston probe was designed and implemented for SThM measurements in 1994 [12], and it was commercialized by Bruker®, although they are not commercially available anymore. This commercial probe was used in our group in different works, [33, 37, 48], which will be discussed in Section 4.1. It consists of a 5 µm in diameter core wire alloy of platinum-rhodium (Pt_{90}/Rd_{10}) with a silver shell of 75 µm. Around 200 µm of the Pt_{90}/Rd_{10} core is exposed by an electrochemical etching and bent into a V-shape (see **Figure 2**). This alloy of the core is the thermistor element, and thus sensitive to the heating, and therefore, the changes in the resistance of this filament are monitored during the scanning of the sample. A mirror for optical beam detection is stuck to the probe by means of an aluminum-coated tape, stacked across the arms of the cantilever, allowing detecting the cantilever deflection by an AFM system. With this kind of probes, for example, memory alloys based on structural transformation have been investigated, such as the studies on the thermal conductivity of NiTi microstructures through their phase transitions carried out by Chirtoc et al. [49]. Moreover, depending on the operation mode implemented during the experiment, not only thermal conductivity but also the Seebeck

coefficient can be measured, as recently published in Refs. [33, 50], working in contact mode. Also, recent publications dealing with Wollaston probes are focused in the quantification of the thermal parameters by studying the theoretical heat transfer models in noncontact mode [51].

Among the advantages to use a Wollaston probe for thermal thin film characterization, it is worth mentioning that they have been used for a long time, and consequently, they are quite well known and they have been extensively used for heat transfer investigation. There are several contributions that analyze theoretically and analytically their behavior. The calibration processes and data reduction can be simplified as it was done in [33] for a scanning hot probe. Besides, these probes can be useful in case that spatial resolution of no more than a few microns is required, or if thermal and topographic images are not desired, since these probes can be easily implemented in a piezoelectric system, acting as thermometer and heater for different applications to perform thermal analysis with a simple experimental setup and fast data acquisition time.

Nevertheless, the reproducibility and the repetition of the experiments can result complicated, given that not only these probes have bending problems of the exposed core, but also the V-shape can change after certain uses or number of scans (as it can be seen in **Figure 2c**). Another disadvantage is that, as far as we know, currently, there are no companies that

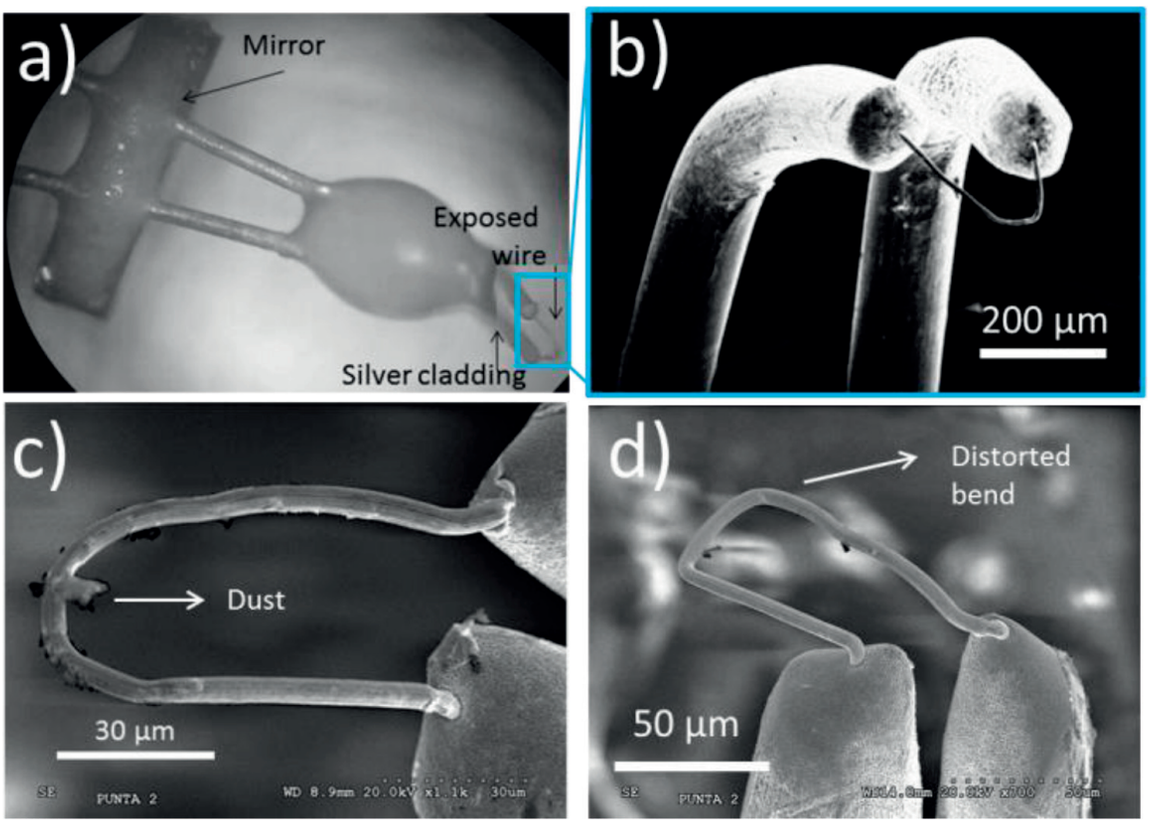

Figure 2. Different images of Wollaston wire probes used in our measurements, where the exposed Pt_{90}/Rd_{10} core bent in a V-shape can be clearly seen, with increasing magnifications from an optical microscope image in (a) with a complete view of the probe with the mirror and the silver legs to (b), where a scanning electron microscope (SEM) detail of the exposed core with a V-shape can be seen. SEM images (c) and (d) show a Wollaston probe after several uses, presenting dust attached to the wire in (c) and a distorted shape in (d).

commercialize these probes, and thus, the only way to use these probes for thermal experiments nowadays is to fabricate them in the laboratory.

2.2.2. Microfabricated metal thin film probes

These types of probes are specially designed for contact mode. They use a thin metal film (of about 50 nm thick) as thermistor element. This film is located near the apex of the tip, and the cantilever is made of silicon dioxide (SiO_2) or silicon nitride (Si_3N_4). The probe has two current limiters of nickel chromium and gold pads to perform the electrical connection. The tip height is usually around 10 μm to maximize the separation between cantilever and sample as a way to avoid heat losses by the cantilever-sample interaction. In the images of **Figure 3**, we can see a microfabricated Pd/Si_3N_4–commercialized by Bruker® and used in our group to perform thermal conductivity characterization of films, as it will be shown in Section 4.

One of the main advantages of using these types of probes is the high thermal and topographic resolution that can be achieved. Also, the cutoff frequency when the probe is heated in AC mode is higher in microfabricated probes than in Wollaston wire probes, as it was reported in [24]. In the same works, the authors highlighted that image acquisition time could be reduced

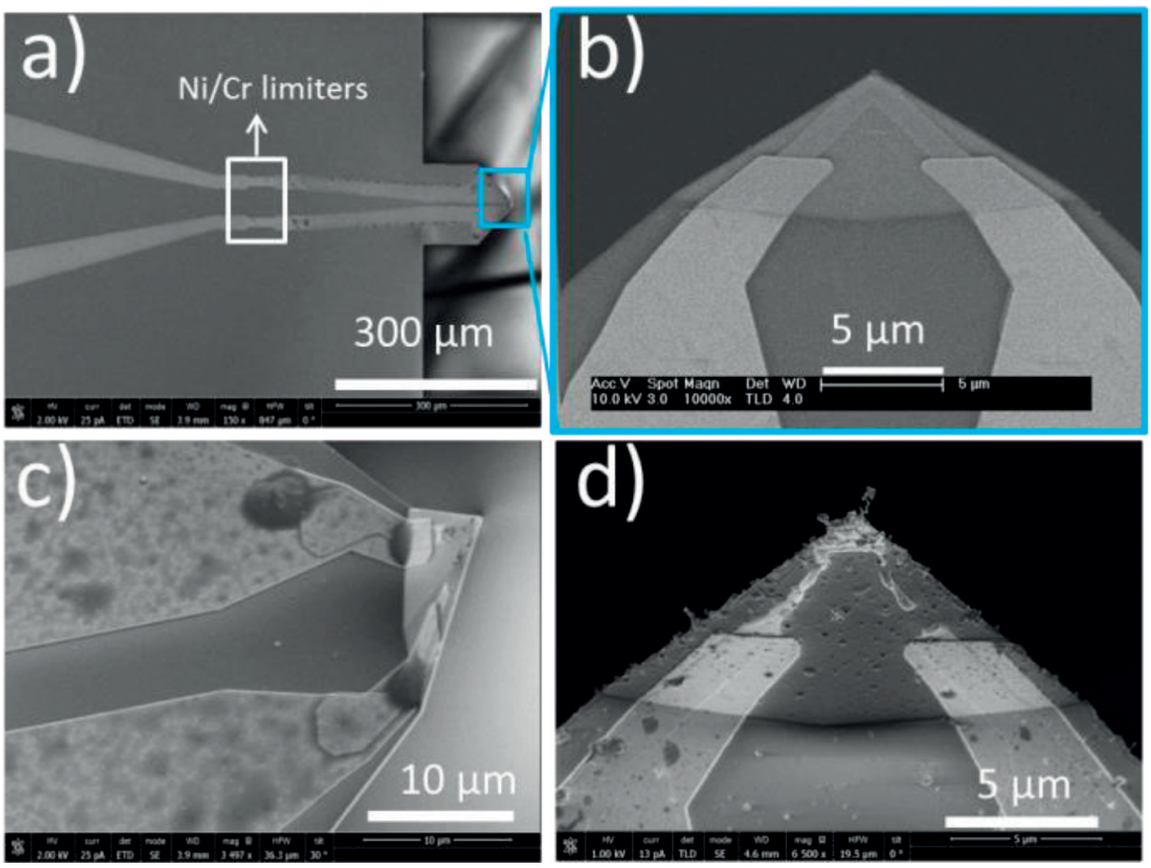

Figure 3. Different scanning electron microscope (SEM) images of a microfabricated Pd/Si_3N_4–commercialized by Bruker® used in our measurements, with increasing magnifications from (a) to (b). Images (c) and (d) show probes where the Pd film of the tip has been removed after electrical breakdown. The angle of the tip can also be clearly seen in (c).

from 1 h in the case of using a Wollaston probe to only 6 min when using a Pd/SiO_2 probe, for an image of 256 × 256 points.

Among the drawbacks that these probes have, one should mention that they are highly static sensitive, so it is not recommended to measure their electrical resistance with conventional resistance meters. Instead, a very careful management is recommended to avoid electrically breaking the probe. In **Figure 3d,** it is shown how the probe looks when the Pd film has been removed, which can occur due to its high static sensitivity. Another disadvantage, when compared with Wollaston wire probes, is the price, which comes from the fact that this is a microfabricated and highly specialized probe. Finally, it is worth mentioning that implementing a heat model for these kinds of probes is also an issue, apart from the calibration steps that have to be done in the probe prior to measure with them. In order to calibrate each probe, many geometrical parameters and material properties must be taken into account to fix the calibration curves, as it is shown in Ref. [29], for instance.

2.2.3. Microfabricated semiconductor probes

In the case of these microfabricated probes, the most used semiconductor material is silicon, which are micromachined in a U-shape, that consists of a low doped platform, which will act

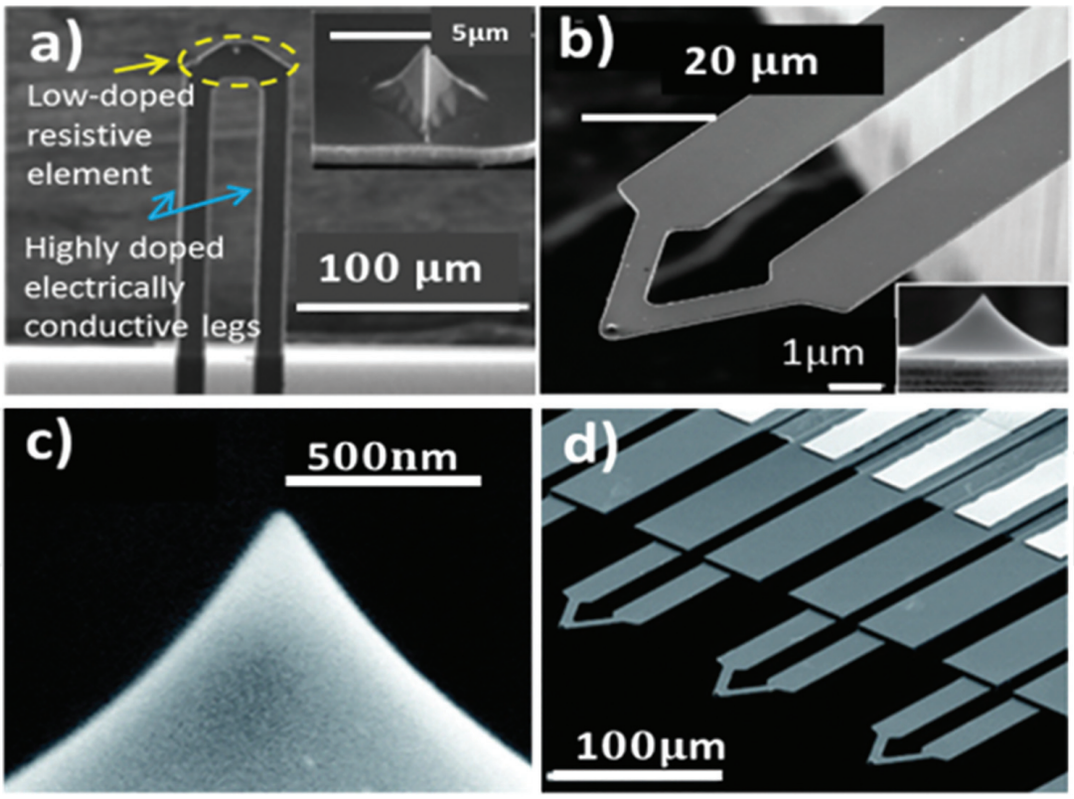

Figure 4. Scanning electron microscope images of microfabricated semiconductor probes, showing different magnifications in the case of (a) pyramidal and (b), (c) conical SEM image in (d) is a part of a whole array of microfabricated cantilevers; (a) is taken from Ref. [56] and (b) is taken from Ref. [57], and (c) and (d) from [58].

as the resistive element (heater) and two highly doped silicon microlegs. Then, the tip is mounted on the resistive element, with a conical [52] or pyramidal [53] shape and curvature radius as low as 10 nm (achieving 100 nm in spatial resolution). The fabrication of these tips is based on microelectronics processes, and thus, batches of sharp probes can be fabricated (see **Figure 4**). These probes were first developed for high-speed nanoscale lithography applications and data-storage systems by IBM, but working in active mode, nanothermal analysis can be performed [54].

The main advantages of these probes are, as it was mentioned before, is the high resolution that can be achieved, allowing even a three-dimensional analysis of nanoscale confinement of certain effects, such as phase transitions (which is not possible when using Wollaston probes, for instance) [53], serving as a highly localized heat source. Moreover, given that they can be produced with scalable fabrication methods, predictable and repeatable thermal parameters in all of them can be produced, along with an important cost reduction. Finally, another relevant benefit of these doped silicon probes is that they can be used in biological media, as in Ref. [55], where they were used to differentiate molecules based on their different heat conductivities.

As far as disadvantages when using these probes for thermal measurements, one has to take into account that they are mainly used for nanolithography and data storage, given that they can deliver up to 1000°C. This reverts to a difficult analysis of the experimental data obtained, given the high thermal contact resistances at the end of the tip, as shown when measuring thin films of polystyrene [53]. Another difficulty for their use in thermal conductivity characterization is that the variation of their electrical resistance cannot be completely described by a linear relation with temperature [56], as it could be done in the previous cases, which further complicates the qualitative measurements.

3. Heating methods with thermistor probes

From now on, we are going to focus on SThM measurements where the local temperature and thermal conductivity of the films are extracted using a thermistor probe. In such a way, while scanning the surface of the sample, the probe can be used as a nanoscale thermometer, as in passive mode operation. But as we saw in Section 2, the probe, if used in active mode, behaves not only as a thermometer but also as a heater. Therefore, if one measures the voltage drop across the probe while a known current passes through it, or if a Wheatstone bridge is used to detect the changes in the resistance of the probe, the actual temperature of the probe can be known, after certain calibration steps. Both of these modes, active or passive, allow the performance of measurements heating the probe with a direct (DC) or an alternate current (AC). The use of an AC current has the advantage of a high signal-to-noise ratio, mainly when combined with lock-in detection, and it also allows the use of the 3ω-SThM technique. Nevertheless, DC heating mode has the advantage of allowing an analytical model analysis of the thermal signal recoiled. A brief overview of the thermal transport models implied in both DC and AC to extract the thermal conductivity with thermistor probes will be discussed next.

3.1. Direct current heating mode

Experimental SThM measurements performed in DC mode can be treated by analytical models to extract the thermal transport properties of the samples. In the case of measuring thin films, several parameters such as the thickness of the film and the influence of the substrate must be taken into account, apart from other general parameters of the measurement system, such as the geometry of the probe, the heat transfer exchange radius, among others. In order to theoretically model the experimental setup when the probe is heated in DC mode, one can simulate the tip by a fin of length L (which corresponds to half of the probe length) and apply the steady-state heat transfer equation when this fin is heated. A detailed explanation of this model is shown by Borca-Tasciuc in [59]. Here, we will give a brief description of the model, starting with the heat transfer equation that has to be fulfilled:

$$\frac{d^2T_P^*}{dx^2} - \left(\frac{2h_{eff}}{\lambda_P r} - \frac{\rho_0 I^2 \beta_P}{\lambda_P A_P^2}\right) T_P^* + \frac{\rho_0 I^2}{\lambda_P A_P^2} = 0 \tag{1}$$

where the index P refers to the probe, $T_P^* = T_P(x) - T_0$, λ is the thermal conductivity, A is the total cross-sectional area, ρ_0 is the electrical resistivity, I corresponds to the root-mean-square electrical current applied to the probe, β is the temperature coefficient of the resistance; $h_{eff} = h + 4\varepsilon\sigma T_0^3$ and hence, h is the convective heat transfer coefficient in air, ε is the emissivity of the probe, σ is the Stefan-Boltzmann constant, and T_0 is the ambient temperature.

In order to obtain an analytical solution for Eq. (1), one has to assume certain boundary conditions, such as keeping the end of the probe at ambient temperature. Also, the geometric characteristics of the probe have to be known and uniform temperature distribution at the tip region has to be assumed. Then, an expression for the average temperature of the probe can be obtained as:

$$T_{av,P}^* = \frac{1}{L}\int_0^L T_P^* dx = T_{DC-av,P} - T_0 \tag{2}$$

where $T_{DC-av,P}$ is the DC average temperature of the probe. Then, the thermal resistance of the probe can be expressed as $R_P^{th} = T_{av,P}^* / \left(I^2 R_{ele,P}\right)$, being $R_{ele.P}$ the electrical resistance of the probe. This ${R_P}^{th}$ can be compared with the experimental effective thermal probe resistance R_{eff}. If the tip is in contact with the film surface, and the thickness of this film is enough to consider it as a semi-infinite medium as far as heat conduction is concerned (bulk or bulk-like thickness), the thermal conductivity of the thin film can then be expressed as:

$$R_S^{th} = \frac{1}{4b\lambda_S} \tag{3}$$

where b is the thermal exchange radius (the area in which the heat transfer is assumed to occur, see **Figure 5**), and R_S^{th} and λ_S are the thermal resistance and the thermal conductivity of the sample, respectively. The limits of the thermal penetration depth are related to the heater

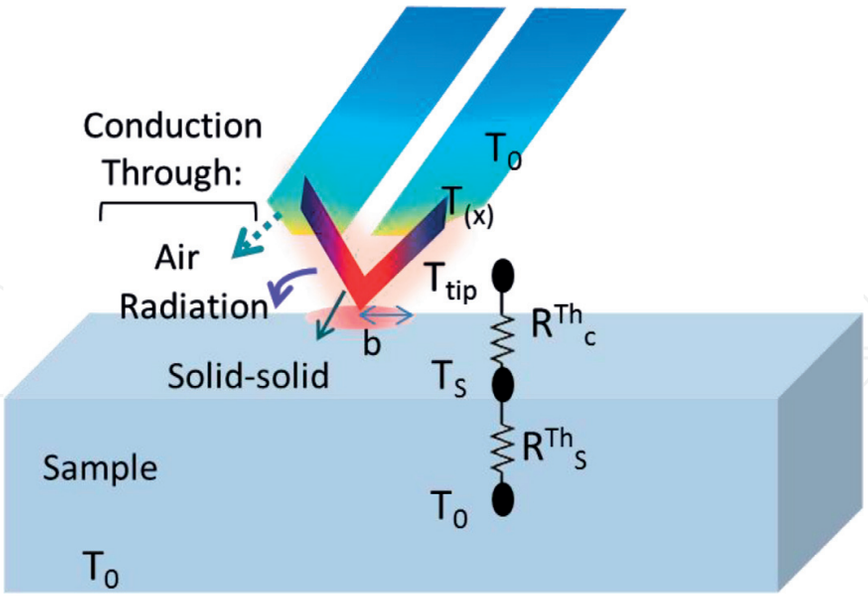

Figure 5. Schemes of the thermal resistance network and thermal interaction between the probe and the sample.

exchange radius, and for the case of having a metal stripe as a heater, as Cahill described in the solution of the diffusion equation for the 3ω method [60], if the sample is a thin film deposited on a substrate, this film must have at least five times the width of the metal heater to avoid influence from the substrate. In another case, that is, if the film is thinner, this expression should be modified to take into account the substrate. Instead, a multilayer structure may be taken into account such as described in [59] by Borca-Tasciuc. The thermal conductivity can be then determined using the simplest case of series thermal resistances network of a film and a substrate, assuming 1D heat transfer through the thickness of the film, if the thermal contact parameters b and R_S^{th} are known (see **Figure 5**). The modified expression for our case results

$$R_S^{th} = \frac{1}{4b\lambda_{Sub}} + \frac{t_f}{\pi b^2 \lambda_f} \tag{4}$$

where t_f is the film thickness and λ_{Sub} and λ_f are the thermal conductivities of the substrate and the film, respectively. In such a way, an analytic solution to extract the thermal conductivity of the film under study, λ_f, from the SThM measurements is obtained.

3.2. Alternating current heating mode

It is worth mentioning that AC heating is more workable with microfabricated probes, due to their smaller thermal mass and higher cutoff frequency when compared with Wollaston probes [59]. Then, in this case, if the thermistor probe is heated with an AC signal, the resulting temperature is a contribution of both a DC and AC profiles. If we define the AC current as $I(t) = I_0 \cos(\omega t)$, the temperature amplitude produced by Joule heating is related to the electrical resistance of the probe and it can be expressed as:

$$T_{2\omega,av} = \frac{2V_{3\omega,tip}}{I_0 R_{ele}\beta_P} \tag{5}$$

where the $V_{3\omega,tip}$ is the 3ω voltage component experimentally measured and β_p is temperature coefficient of the resistance of the probe. The heat transfer equations of the probe for this AC temperature field should be developed taking into account the differences in the cross-sectional areas for the heat and current flow. In the work of 2005, Lefèvre and Volz [21] presented a theoretical model on AC heating, along with experimental results to validate it. In this study, it was clear that a Wollaston-size wire does not allow reaching a transient thermal behavior, which is needed for the classical 3ω method with a hot strip. In this study, they based the model on the transient fin equation, including a source term due to the joule dissipation. Several years later, based on the previous model, Puyoo et al. [29] presented a thermal description for the probe behavior under air conditions in both out-of-contact and in-contact modes. In this case, they separated the cross-sectional areas corresponding to the probe and that of the metallic Pd film (the heating element), with the aim to identify the geometric parameters depending on the probe type. In this respect, the corresponding heat equation solved in the Fourier space is:

$$\frac{\mathrm{d}^2 T_{2\omega,P}}{\mathrm{dx}^2} - \left(\frac{2i\omega}{\alpha_P} + \frac{hp_P}{\lambda_P A_P}\right) T_{2\omega,P} + \frac{\rho I_0^2}{2\lambda_P A_P A_M} = 0 \tag{6}$$

where the index P denotes the probe, p is the perimeter and A is the total cross-section area of the probe, A_M is the cross-sectional area of the metallic film of the heater element, ρ is the electrical resistivity, I_0 is the current amplitude, h *is* the effective convective heat transfer coefficient in air, α and λ represent the thermal diffusivity and the thermal conductivity, respectively. It is important to remark that thermal radiation effects are negligible due to the small amplitude of AC temperature, as it was pointed by Borca-Tasciuc [59]. When $\omega \to 0$, the equation of AC heating becomes a simplified DC heating equation, with no transient contribution. If now one considers that the heat flux takes place only at the apex of the tip, the metal pads of the tip can be taken as thermal sinks and the temperature variation at this junction can be disregarded. Taking all these into account, when the probe is in contact, the heat flux can be then defined as:

$$-\lambda_{\mathrm{P}} \mathrm{A}_{\mathrm{P}} \left.\frac{d\mathrm{T}_{2\omega,\mathrm{P}}}{dx}\right|_{x=L} = \frac{\mathrm{T}_{2\omega,\mathrm{P}}|_{x=L}}{R_{eq}^{th}} \tag{7}$$

L being the length of the metallic film and the R_{eq}^{th} the equivalent thermal resistance, which is the contribution of the thermal resistances in series from both the tip-sample contact, R_C^{th}, and the thermal resistance of the sample, R_S^{th}. When applying the boundary conditions for contact or out of contact cases, the transient fin equation can be solved (details can be found in [21, 29, 59]) and an analytical expression for the 2ω varying tip temperature can be obtained. Then, the final expression for the heat flux, assuming that the sample is a semi-infinite body heated by a semispherical heat source of radius b becomes

$$Q_S = 2\pi b \lambda_S T_{2\omega,S} \left(1 + b\sqrt{\frac{2i\omega}{\alpha_S}}\right) \tag{8}$$

where Q is the heat transfer rate and the index S refers to the sample. With this expression, it is possible to obtain parameters such as the thermal conductivity (λ_S) of the thin film sample analyzed.

4. Thin film measurements by SThM

As it has been seen along this chapter, the SThM technique is quite suitable for the measurement of thermal properties of thin films. In the literature, one can find many examples, such as the work from Oesterschulze et al. in 1996 [61], where they used a combination of a photothermal SThM and STM setup. In such a way, they obtained at the same time the topography, the DC image of the temperature, the AC temperature amplitude, and the phase image of thin polycrystalline diamond films. Thanks to the thermal images, some features that were not visible in the topographical image could be studied. In this case, the thermovoltage map was correlated with the single crystallites, where thermovoltage was constant. On the side planes, the decreasing of thermovoltage was related to the laminar structures parallel to the edges of the top plane. More recent works on thin film characterization by SThM [62] deal with the correlation of the thermal properties of $BaTiO_3$ thin films with their morphology. In order to give further examples of the application of the SThM technique, we will discuss next some examples of measurements performed in thermoelectric thin films from our group.

4.1. Thermoelectric thin film measurements: Wollaston probes

To perform measurements with a Wollaston probe in thin films, a circuit as the one shown in **Figure 6a** was implemented. Prior to the measurement, a thorough calibration of the system

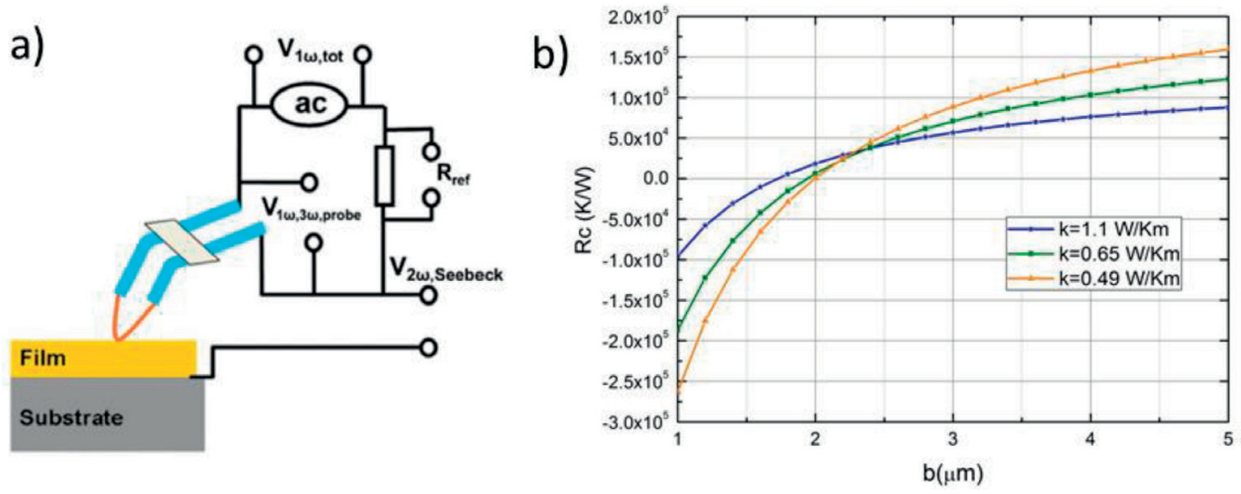

Figure 6. (a) Electrical circuit used for the measurement with the Wollaston probe (reproduced from [33]) and (b) calibration curves for obtaining R_c and b (from [37]).

was necessary. This calibration consists of measuring three different samples of known thermal conductivity to determine the thermal exchange radius (b) and the thermal contact resistance between the tip and the film (R_C), as it is shown in **Figure 6b**. The measurements were performed in contact mode and in air conditions. In these cases, no scanning was performed to obtain thermal images, but the AFM system was used in order to position the tip on the surface of the film. The values obtained could be influenced by the substrate, so a further analysis of the results with COMSOL® software was necessary to extract the information of the thin film in those cases. With this technique, the thermal conductivity of a variety of thin films was characterized in the work by Wilson et al. [33]: SiGe (1.22 ± 0.21 W/m·K) and Te films (0.79 ± 0.04 W/m·K) on glass, Au film on silicon (104.2 ± 67.4 W/m·K), and polymer films of PCDTBT on glass substrates, both Fe-doped (1.03 ± 0.15 W/m·K) and undoped (0.25 ± 0.21 W/m·K). These values show a wide range of thermal conductivities that can be measured when the calibration is carefully made, and the appropriate models are taken into account. Following these results, the thermal conductivity of a large area of a nanomesh $Si_{0.8}Ge_{0.2}$ film was also characterized [37]. In this case, the nanomesh structure produced a reduction on the thermal conductivity with the decrease in the diameter of the pores forming the mesh, from 1.54 W/m·K for around 300 nm in diameter pores to a value of 0.55 W/m·K for pores of approximately 30 nm in diameter. This result is quite relevant for the field of thermoelectricity, given that the reduction in thermal conductivity via nanostructuration without affecting the other transport properties is a way to enhance thermoelectric efficiency. The accurate measurement of the actual reduction in thermal conductivity in thin films provides a way to really understand the thermal conductivity at the nanoscale.

4.2. Thermoelectric thin film measurements: microfabricated probes

In order to enhance the thermal image resolution to explore different thermoelectric thin films and study their nanostructure, it was necessary to change the probes from Wollaston to microfabricated probes. In this case, the electrical circuit used, which can be seen in **Figure 7a**, consists of a home-made Wheatstone bridge, which will be used to detect the resistance changes of the probe, connected to a lock-in amplifier from Zurich Instruments®. Finally, the lock-in is connected with an AFM from Nanotec Electronica®, in which the tip is mounted. In this way, topographic and thermal images of the sample are simultaneously obtained. The thermal conductivity was obtained using an active mode at constant current and under ambient conditions. To obtain the geometrical parameters of the probe and its thermal response, it is necessary to perform a prior calibration both in ambient conditions and in high vacuum (10^{-5} mbar), as it was mentioned in Section 2.2.2 [29]. In order to analyze the thermal response of the probe in out-of-contact mode, one varies the applied frequency while detecting the 3ω voltage, both in vacuum and in atmospheric conditions, obtaining a graph such as that shown in **Figure 7b**. This has to be made with special care to avoid any electrical breakdown of the tip. These data have to be fixed with a theoretical curve, which takes into account the geometrical parameters of the probe (length, thickness of the Pd and the SiN_x, the convective coefficient, electrical resistance, temperature coefficient resistance, etc.). With these geometrical parameters fixed, a different model is used to determine the equivalent thermal response of the tip, R_{eq}, as a function of the 3ω voltage. Finally, samples of known thermal conductivity [33] are

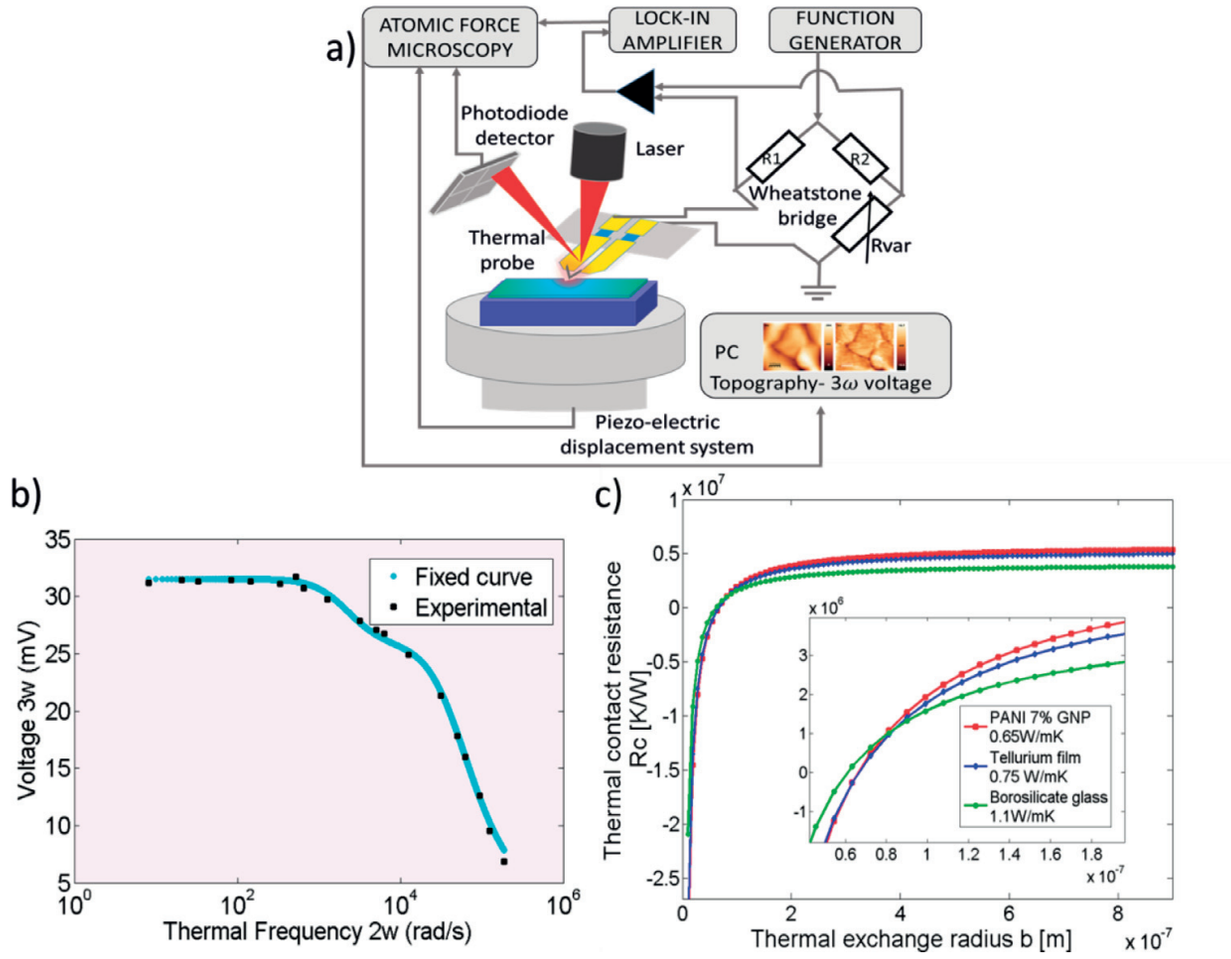

Figure 7. (a) Scheme of the experimental setup and electrical circuit with the Wheatstone bridge, (b) experimental data and model adjustment of the measurements of the 3ω response of the probe versus thermal frequency at atmospheric conditions (from [41]), and (c) calibration curves to extract R_c and b.

measured in contact mode and in ambient conditions, and the obtained 3ω is modeled with a further simulation, which takes into account all the parameters previously obtained, along with the unknown thermal exchange radius, *b*, and thermal constant resistance, *Rc*, obtaining curves as those shown **Figure 7c**. From the cross-point of these graphs, *b*, and *Rc* are obtained for this particular tip.

This experimental setup was successfully implemented to obtain thermal images of different thermoelectric films and to determine their thermal conductivity. For instance, in the work of Perez-Taborda et al., a novel fabrication method to obtain thin films Cu_2Se with high control over the stoichiometry was achieved [40]. In this case, the thermal conductivity at room temperature under ambient conditions obtained via SThM measurements, arouse a value as low as 0.8 ± 0.1 W/m·K, which results in a TE figure of merit of 0.4. A detail on these measurements can be found in **Figure 8**, where the topographic and thermal images can be seen. Apart from the good resolution of the images, the most important feature shown in these images is that the $V_{3\omega}$ voltage is not influenced by the artifacts or topographic effects. This can be seen in **Figure 7c** and **f** when numbers 1 and 2 located inside of the images are compared.

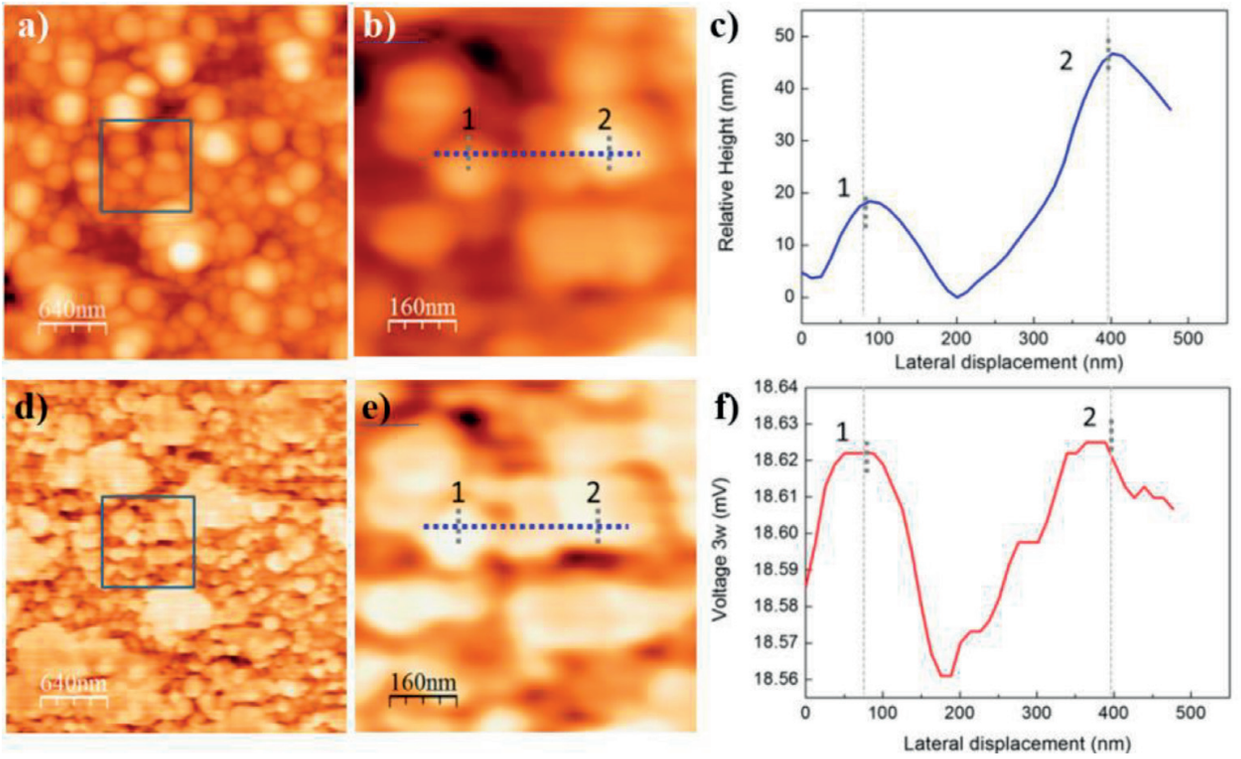

Figure 8. (a and b) Topography images at two different scales, and (c) shows a profile along the blue line in (b); (d) and (e) show the thermal images at the same scale than (a) and (b); and (f) shows the corresponding profile along the blue line in (e). Note that numbers 1 and 2 in these profiles indicate the same lateral displacement position for topography and $V_{3\omega}$ (images (a) and (d) are adapted from Ref. [40]).

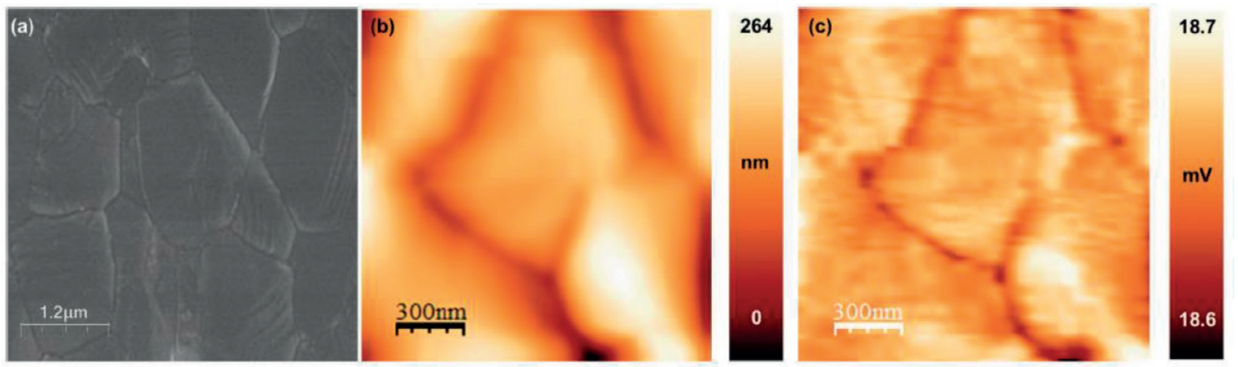

Figure 9. (a) SEM, (b) topographical, and (c) thermal map images obtained with SThM using a Pd/Si_3N_4 microfabricated probe (from [41]).

The $V_{3\omega}$ voltage is quite homogeneous along the surface of the film, and it is not much influenced by the topographical height. It is also worth mentioning that the highest values in $V_{3\omega}$ are the regions with the lowest thermal conductivity.

Microfabricated probes were also used for the measurement of Ag_2Se films, which presented a different morphology of bigger grains than in the previous case, which does not affect the thermal conductivity (see **Figure 9**). These films, of around 700 nm in thickness, presented in

[41], had a highly reduced thermal conductivity (0.64 ± 0.1 W/m·K) when compared to the same material in bulk (reported as 1.5 W/m·K [63]). In this case, this reduction in the thermal conductivity, along with the good measured transport properties, arouses in a thin film with a TE Figure of Merit (zT) of 1.2 at room temperature, comparable or even higher than other thermoelectric materials that are commonly used for thermoelectric devices. It is worth noting that this excellent value comes from the nanostructuration of the material into a thin film along with a fabrication method that provides high control over its quality. Therefore, the accurate characterization of the thermal conductivity was of the utmost importance to confirm the optimization due to nanoscale thermal transport modification.

5. Summary and outlook

The thermal conductivity characterization and local temperature measurements at the nanoscale of thin films are of the utmost importance in a great number of fields, such as in electronics, where heat management is vital for the final efficiency of the devices, solar cells, coatings, etc. Among those fields, thermoelectricity stands out, given that the reduction in the thermal conductivity due to nanostructuration is one of the main objectives nowadays to increase the thermoelectric performance of the materials.

Along this chapter, we have presented the SThM method applied to the measurement of thermal properties of thin films. The main advantages of this method are the high resolution (in the nanometer scale), the possibility to simultaneously obtain the topography and the thermal image of the surface, and, from the experimental point of view, the sample preparation process is easily compared with other thermal characterization techniques. The SThM technique was first implemented in an AFM in 1993, and since then a great deal of effort has been devoted to understanding in depth both the heat transfer at the nanoscale and the phenomena that have to be taken into account in these kinds of measurements. After a review of the historical advances related to the development of the SThM, experimental details about the operational modes and different kinds of probes were discussed. Then, the theories behind the heating models involved in a certain type of probes were briefly introduced. At the end of the chapter, results obtained in our group on the thermal conductivity of thermoelectric thin films performed with SThM were shown, demonstrating the suitability of this technique for these kinds of measurements.

One of the most appealing future directions based on these techniques would be the use of multipurpose probes to obtain, at the nanoscale, simultaneous information about electrical, thermal, chemical and mechanical properties, among others. The main challenge would then be the understanding of the different transport phenomena at the nanoscale, and how to physically represent the different interactions between the probes and the samples. Therefore, the development of more complex models, along with the evolution of micro- and nanofabrication techniques, opens the door to a new blooming of methods based on SThM for a full characterization of thin film properties at the nanoscale.

Acknowledgments

The authors acknowledge the financial support of the Intramural INFANTE, and MAT2017-86450-C4-3-R, as well as the service from the MiNa Laboratory at IMN, and funding from CM (project SpaceTec, S2013/ICE2822), MINECO (project CSIC13-4E-1794), and EU (FEDER, FSE). O.C.C. acknowledges the funding of the Ramón y Cajal program (MINECO).

Conflict of interest

The authors declare no conflict of interest.

Author details

Liliana Vera-Londono[1], Olga Caballero-Calero[1], Jaime Andrés Pérez-Taborda[1,2] and Marisol Martín-González[1]*

*Address all correspondence to: marisol@imn.cnm.csic.es

1 IMN-Instituto de Micro y Nanotecnología, IMN-CNM, CSIC (CEI UAM+CSIC), Madrid, Spain

2 Department of Electrical and Electronic Engineering and Centro de Microelectrónica (CMUA) Universidad de los Andes, Bogotá, Colombia

References

[1] Franklin AD. Nanomaterials in transistors: From high-performance to thin-film applications. Science. 2015;**349**:aab2750

[2] Lee TD, Ebong AU. A review of thin film solar cell technologies and challenges. Renewable and Sustainable Energy Reviews. 2017;**70**:1286-1297

[3] Forrest SR. The path to ubiquitous and low-cost organic electronic appliances on plastic. Nature. 2004;**428**:911

[4] Chowdhury I, Prasher R, Lofgreen K, Chrysler G, Narasimhan S, Mahajan R, et al. On-chip cooling by superlattice-based thin-film thermoelectrics. Nature Nanotechnology. 2009;**4**:235

[5] Binnig G, Quate CF, Gerber C. Atomic force microscope. Physical Review Letters. 1986;**56**:930

[6] Williams C, Wickramasinghe H. Scanning thermal profiler. Microelectronic Engineering. 1986;**5**:509-513

[7] Weaver J, Walpita L, Wickramasinghe H. Optical absorption microscopy and spectroscopy with nanometre resolution. Nature. 1989;**342**:783

[8] Williams CC, Wickramasinghe H. Microscopy of chemical-potential variations on an atomic scale. Nature. 1990;**344**:317

[9] Nonnenmacher M, O'Boyle M, Wickramasinghe HK. Kelvin probe force microscopy. Applied Physics Letters. 1991;**58**:2921-2923

[10] Nonnenmacher M, Wickramasinghe H. Scanning probe microscopy of thermal conductivity and subsurface properties. Applied Physics Letters. 1992;**61**:168-170

[11] Majumdar A, Carrejo J, Lai J. Thermal imaging using the atomic force microscope. Applied Physics Letters. 1993;**62**:2501-2503

[12] Pylkki RJ, Moyer PJ, West PE. Scanning near-field optical microscopy and scanning thermal microscopy. Japanese Journal of Applied Physics. 1994;**33**:3785

[13] Majumdar A, Lai J, Chandrachood M, Nakabeppu O, Wu Y, Shi Z. Thermal imaging by atomic force microscopy using thermocouple cantilever probes. Review of Scientific Instruments. 1995;**66**:3584-3592

[14] Hammiche A, Pollock H, Song M, Hourston D. Sub-surface imaging by scanning thermal microscopy. Measurement Science and Technology. 1996;**7**:142

[15] Kölzer J, Oesterschulze E, Deboy G. Thermal imaging and measurement techniques for electronic materials and devices. Microelectronic Engineering. 1996;**31**:251-270

[16] Gmelin E, Fischer R, Stitzinger R. Sub-micrometer thermal physics–an overview on SThM techniques1. Thermochimica Acta. 1998;**310**:1-17

[17] Majumdar A. Scanning thermal microscopy. Annual Review of Materials Science. 1999;**29**: 505-585

[18] Fiege GBM, Altes A, Heiderhoff R, Balk LJ. Quantitative thermal conductivity measurements with nanometre resolution. Journal of Physics D: Applied Physics. 1999;**32**:L13

[19] Cahill DG, Pohl RO. Thermal conductivity of amorphous solids above the plateau. Physical Review B. 1987;**35**:4067

[20] Lefevre S, Saulnier J-B, Fuentes C, Volz S. Probe calibration of the scanning thermal microscope in the AC mode. Superlattices and Microstructures. 2004;**35**:283-288

[21] Lefèvre S, Volz S. 3ω-scanning thermal microscope. Review of Scientific Instruments. 2005;**76**:033701

[22] Chapuis P-O, Saha SK, Volz S. Quantitative 3w-scanning thermal microscopy: Modelling the AC/DC coupling and the sample heat conduction. In: THERMINIC 2006. 2006. pp. 210-213

[23] Lefèvre S, Volz S, Chapuis P-O. Nanoscale heat transfer at contact between a hot tip and a substrate. International Journal of Heat and Mass Transfer. 2006;**49**:251-258

[24] Puyoo E, Grauby S, Rampnoux J-M, Rouvière E, Dilhaire S. Thermal exchange radius measurement: Application to nanowire thermal imaging. Review of Scientific Instruments. 2010;**81**:073701

[25] Shi L, Majumdar A. Thermal transport mechanisms at nanoscale point contacts. Journal of Heat Transfer. 2002;**124**:329-337

[26] Lefevre S, Volz S, Saulnier J-B, Fuentes C, Trannoy N. Thermal conductivity calibration for hot wire based dc scanning thermal microscopy. Review of Scientific Instruments. 2003;**74**: 2418-2423

[27] David L, Gomes S, Raynaud M. Modelling for the thermal characterization of solid materials by dc scanning thermal microscopy. Journal of Physics D: Applied Physics. 2007;**40**:4337

[28] Kim K, Chung J, Won J, Kwon O, Lee JS, Park SH, et al. Quantitative scanning thermal microscopy using double scan technique. Applied Physics Letters. 2008;**93**:203115

[29] Puyoo E, Grauby S, Rampnoux J-M, Rouvière E, Dilhaire S. Scanning thermal microscopy of individual silicon nanowires. Journal of Applied Physics. 2011;**109**:024302

[30] Muñoz Rojo M, Grauby S, Rampnoux J-M, Caballero-Calero O, Martin-Gonzalez M, Dilhaire S. Fabrication of Bi_2Te_3 nanowire arrays and thermal conductivity measurement by 3ω-scanning thermal microscopy. Journal of Applied Physics. 2013;**113**:054308

[31] Shi L, Plyasunov S, Bachtold A, McEuen PL, Majumdar A. Scanning thermal microscopy of carbon nanotubes using batch-fabricated probes. Applied Physics Letters. 2000;**77**: 4295-4297

[32] Nazarenko M, Rosamond MC, Gallant AJ, Kolosov OV, Dubrovskii VG, Zeze DA. A simplified model to estimate thermal resistance between carbon nanotube and sample in scanning thermal microscopy. Journal of Physics D: Applied Physics. 2017;**50**:494004

[33] Wilson AA, Rojo MM, Abad B, Perez JA, Maiz J, Schomacker J, et al. Thermal conductivity measurements of high and low thermal conductivity films using a scanning hot probe method in the 3ω mode and novel calibration strategies. Nanoscale. 2015;**7**:15404-15412

[34] Bosse J, Timofeeva M, Tovee P, Robinson B, Huey B, Kolosov O. Nanothermal characterization of amorphous and crystalline phases in chalcogenide thin films with scanning thermal microscopy. Journal of Applied Physics. 2014;**116**:134904

[35] Smithe KKH, Krayev AV, Bailey CS, Lee HR, Yalon E, Aslan ÖB, et al. Nanoscale heterogeneities in monolayer $MoSe_2$ revealed by correlated scanning probe microscopy and tip-enhanced raman spectroscopy. ACS Applied Nano Materials. 2018;**1**:572

[36] Martín-González M, Caballero-Calero O, Díaz-Chao P. Nanoengineering thermoelectrics for 21st century: Energy harvesting and other trends in the field. Renewable and Sustainable Energy Reviews. 2013;**24**:288-305

[37] Perez-Taborda JA, Rojo MM, Maiz J, Neophytou N, Martin-Gonzalez M. Ultra-low thermal conductivities in large-area Si-Ge nanomeshes for thermoelectric applications. Scientific Reports. 2016;**6**:32778

[38] Pérez-Taborda JA, Caballero-Calero O, Martín-González M. Silicon-Germanium (SiGe) nanostructures for thermoelectric devices: Recent advances and new approaches to high thermoelectric efficiency. In: New Research on Silicon-Structure, Properties, Technology. United Kingdom: InTech; 2017

[39] Taborda JP, Romero J, Abad B, Muñoz-Rojo M, Mello A, Briones F, et al. Low thermal conductivity and improved thermoelectric performance of nanocrystalline silicon germanium films by sputtering. Nanotechnology. 2016;**27**:175401

[40] Perez-Taborda JA, Vera L, Caballero-Calero O, Lopez EO, Romero JJ, Stroppa DG, et al. Pulsed hybrid reactive magnetron sputtering for high zT Cu_2Se thermoelectric films. Advanced Materials Technologies. 2017;**2**:1700012

[41] Perez-Taborda JA, Caballero-Calero O, Vera-Londono L, Briones F, Martin-Gonzalez M. High thermoelectric zT in n-type silver selenide films at room temperature. Advanced Energy Materials. 2018;**8**:1702024

[42] Kim K, Jeong W, Lee W, Sadat S, Thompson D, Meyhofer E, et al. Quantification of thermal and contact resistances of scanning thermal probes. Applied Physics Letters. 2014;**105**:203107

[43] Shi L, Kwon O, Miner AC, Majumdar A. Design and batch fabrication of probes for sub-100 nm scanning thermal microscopy. Journal of Microelectromechanical Systems. 2001; **10**:370-378

[44] Chae H, Hwang G, Kwon O. Fabrication of scanning thermal microscope probe with ultra-thin oxide tip and demonstration of its enhanced performance. Ultramicroscopy. 2016;**171**:195-203

[45] Roh HH, Lee JS, Kim DL, Park J, Kim K, Kwon O, et al. Novel nanoscale thermal property imaging technique: The 2ω method. I. Principle and the 2ω signal measurement. Journal of Vacuum Science & Technology, B: Microelectronics and Nanometer Structures–Processing, Measurement, and Phenomena. 2006;**24**:2398-2404

[46] Roh HH, Lee JS, Kim DL, Park J, Kim K, Kwon O, et al. Novel nanoscale thermal property imaging technique: The 2ω method. II. Demonstration and comparison. Journal of Vacuum Science & Technology, B: Microelectronics and Nanometer Structures–Processing, Measurement, and Phenomena. 2006;**24**:2405-2411

[47] Cui L, Jeong W, Fernández-Hurtado V, Feist J, García-Vidal FJ, Cuevas JC, et al. Study of radiative heat transfer in Ångström-and nanometre-sized gaps. Nature Communications. 2017;**8**:14479

[48] Rojo MM, Abad B, Manzano C, Torres P, Cartoixà X, Alvarez F, et al. Thermal conductivity of Bi_2Te_3 nanowires: How size affects phonon scattering. Nanoscale. 2017;**9**:6741-6747

[49] Chirtoc M, Gibkes J, Wernhardt R, Pelzl J, Wieck A. Temperature-dependent quantitative 3ω scanning thermal microscopy: Local thermal conductivity changes in NiTi microstructures induced by martensite-austenite phase transition. Review of Scientific Instruments. 2008;**79**:093703

[50] Zhang Y, Hapenciuc CL, Castillo EE, Borca-Tasciuc T, Mehta RJ, Karthik C, et al. A microprobe technique for simultaneously measuring thermal conductivity and Seebeck coefficient of thin films. Applied Physics Letters. 2010;**96**:062107

[51] Wilson AA, Borca-Tasciuc T. Quantifying non-contact tip-sample thermal exchange parameters for accurate scanning thermal microscopy with heated microprobes. Review of Scientific Instruments. 2017;**88**:074903

[52] Despont M, Brugger J, Drechsler U, Dürig U, Häberle W, Lutwyche M, et al. VLSI-NEMS chip for parallel AFM data storage. Sensors and Actuators A: Physical. 2000;**80**:100-107

[53] Nelson B, King W. Measuring material softening with nanoscale spatial resolution using heated silicon probes. Review of Scientific Instruments. 2007;**78**:023702

[54] King WP, Bhatia B, Felts JR, Kim HJ, Kwon B, Lee B, et al. Heated atomic force microscope cantilevers and their applications. Annual Review of Heat Transfer. 2013;**16**:288-326

[55] Haeberle W, Pantea M, Hoerber J. Nanometer-scale heat-conductivity measurements on biological samples. Ultramicroscopy. 2006;**106**:678-686

[56] Gomès S, Assy A, Chapuis PO. Scanning thermal microscopy: A review. Physica Status Solidi. 2015;**212**:477-494

[57] Hu H, Kim HJ, Somnath S. Tip-based nanofabrication for scalable manufacturing. Micromachines. 2017;**8**:90

[58] Seong M, Somnath S, Kim HJ, King WP. Parallel nanoimaging using an array of 30 heated microcantilevers. RSC Advances. 2014;**4**:24747-24754

[59] Borca-Tasciuc T. Scanning probe methods for thermal and thermoelectric property measurements. Annual Review of Heat Transfer. 2013;**16**:211-258

[60] Cahill DG. Thermal conductivity measurement from 30 to 750 K: The 3ω method. Review of Scientific Instruments. 1990;**61**:802-808

[61] Oesterschulze E, Stopka M, Ackermann L, Scholz W, Werner S. Thermal imaging of thin films by scanning thermal microscope. Journal of Vacuum Science & Technology, B: Microelectronics and Nanometer Structures–Processing, Measurement, and Phenomena. 1996;**14**:832-837

[62] Kaźmierczak-Bałata A, Bodzenta J, Krzywiecki M, Juszczyk J, Szmidt J, Firek P. Application of scanning microscopy to study correlation between thermal properties and morphology of $BaTiO_3$ thin films. Thin Solid Films. 2013;**545**:217-221

[63] Day T, Drymiotis F, Zhang T, Rhodes D, Shi X, Chen L, et al. Evaluating the potential for high thermoelectric efficiency of silver selenide. Journal of Materials Chemistry C. 2013;**1**: 7568-7573